ELSEVIER

Fusion Engineering and Design 51–52 (2000) 681–694

Fusion Engineering and Design

www.elsevier.com/locate/fusengdes

Theory and models of material erosion and lifetime during plasma instabilities in a tokamak environment

A. Hassanein [a,*], I. Konkashbaev [a,b]

[a] *Argonne National Laboratory, Energy Technology Division, Building 207, 9700 South Cass Avenue, Argonne, IL 60439, USA*
[b] *Troitsk Institute for Innovation and Fusion Research, Russia*

Abstract

Surface and structural damage to plasma-facing components (PFCs) due to the frequent loss of plasma confinement remains a serious problem for the tokamak reactor concept. The deposited plasma energy causes significant surface erosion, possible structural failure and frequent plasma contamination. Surface damage consists of vaporization, spallation, and liquid splatter of metallic materials. Structural damage includes large temperature increases in structural materials and at the interfaces between surface coatings and structural members. To evaluate the lifetimes of plasma-facing materials and nearby components and to predict the various forms of damage that they experience, comprehensive models (contained in the HEIGHTS computer simulation package) are developed, integrated self-consistently and enhanced. Splashing mechanisms, such as bubble boiling and various liquid magnetohydrodynamic instabilities and brittle destruction mechanisms of non-melting materials, are being examined. The design requirements and implications of plasma-facing and nearby components are discussed, along with recommendations to mitigate and reduce the effects of plasma instabilities on reactor components. © 2000 Published by Elsevier Science B.V.

Keywords: Plasma; Erosion; Materials; Disruptions; Vapour shielding; HEIGHTS

1. Introduction

Interaction of powerful plasma and particle beams — power densities up to hundreds of GW/m^2 and time duration up to tens of ms — with various materials, causes significant damage to exposed target surfaces and nearby components. Investigation of material erosion and damage due to intense energy deposition on target surfaces is essential for many applications: space studies, protection of the earth's surface from colliding asteroids and comets, creation of new sources of radiation, high-energy physics applications, thermonuclear fusion studies, etc. Experimental and theoretical activities in this field move toward the common goal of achieving a better understanding of various plasma/surface interaction phenomena and material properties under extreme conditions of temperature and pressure. An important application of this problem is in future tokamak fusion devices during plasma interaction with plasma-facing materials (PFMs).

* Corresponding author. Tel.: +1-630-2525889; fax: +1-630-2525287.

0920-3796/00/$ - see front matter © 2000 Published by Elsevier Science B.V.
PII: S0920-3796(00)00245-3

Damage to plasma-facing and nearby components as a result of various plasma instabilities that cause loss of plasma confinement remains a major obstacle to a successful tokamak concept. Plasma instabilities can take various forms, such as hard disruptions, which include both thermal and current quench (sometimes producing runaway electrons), edge-localized modes (ELMs) and vertical displacement events (VDEs). The extent of the damage depends on the detailed physics of the disrupting plasma, the physics of plasma/material interactions and the design configuration of plasma-facing components (PFCs). Plasma instabilities, such as hard disruptions, ELMs and VDEs will cause both surface and bulk damage to plasma-facing and structural materials. Surface damage includes high erosion losses from surface vaporization, spallation and melt-layer erosion. Bulk damage includes large temperature increases in structural materials and at the interfaces between surface coatings and structural materials. These large temperature increases will cause high thermal stresses, possible melting and material fatigue and failure. Other bulk effects of some plasma instabilities, particularly those of longer duration such as VDEs and those with deeper deposited energy such as runaway electrons, can cause high heat flux levels at the coolant channels, causing possible burnout of these tubes [1]. In addition to these effects, the transport and redeposition of the eroded surface materials to various locations on plasma-facing and nearby components are of major concern for plasma contamination, for safety (dust inventory hazard) and for successful and prolonged plasma operation following instability events [2]. Fig. 1 illustrates the possible effects of different plasma instabilities on target surfaces and bulk materials.

Four key factors can significantly influence the overall response and erosion lifetime of a PFC as

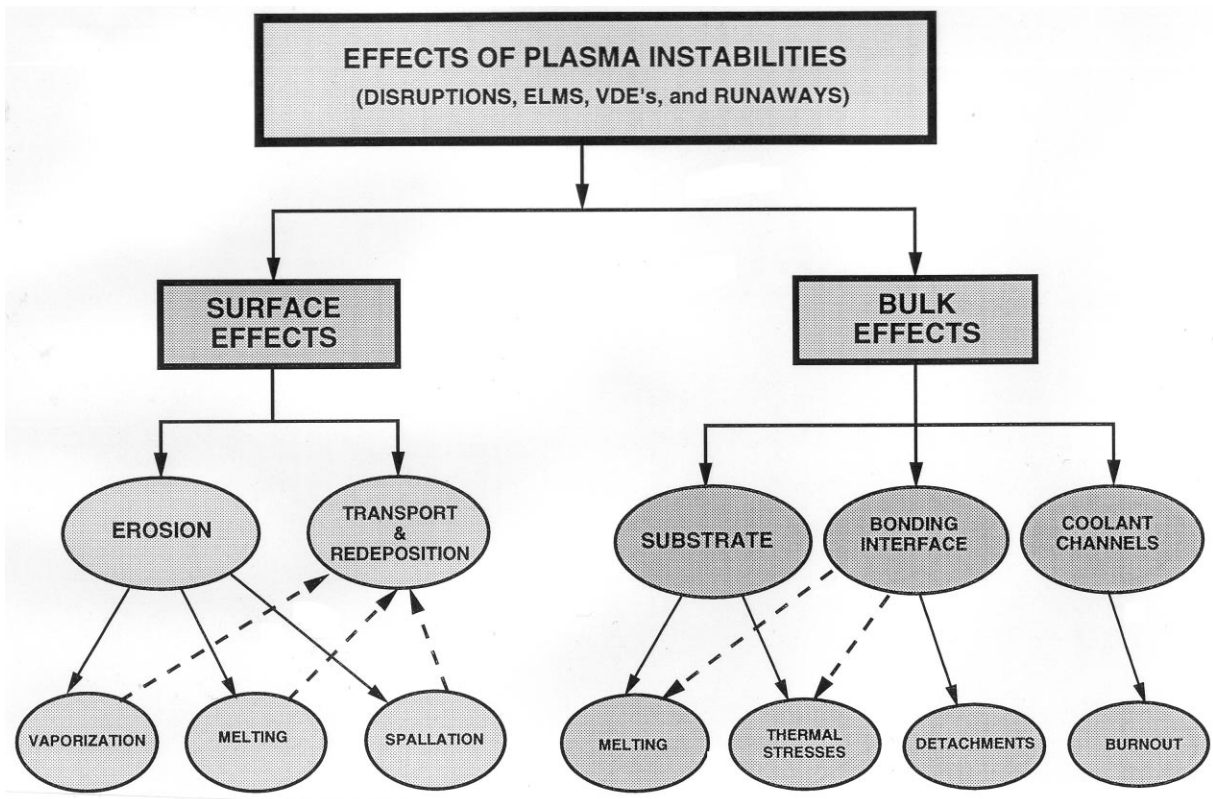

Fig. 1. Effects of plasma instabilities on target materials.

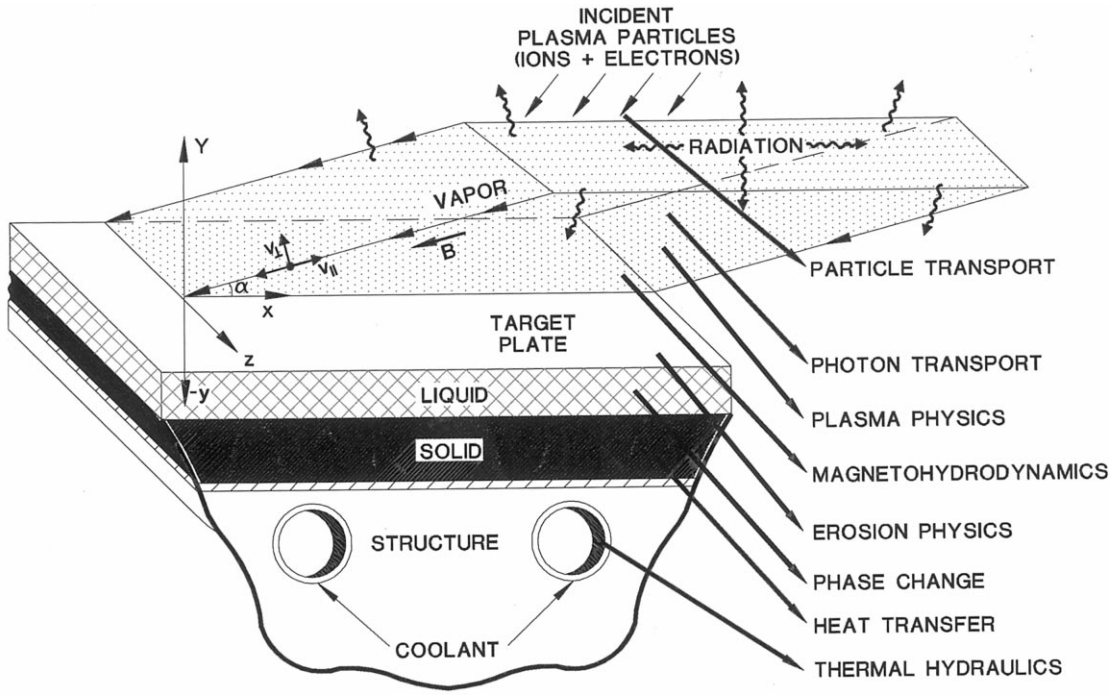

Fig. 2. Schematic illustration of various interaction zones and physics during plasma instabilities.

a result of the intense deposited energy during plasma instabilities. These are: (a) characteristics of particle-energy flow (i.e. particle type, kinetic energy, energy content, deposition time and location) from the scrape-off-layer (SOL) to the divertor plate; (b) characteristics of the vapor cloud that develops from the initial phase of energy deposition on target materials and its turbulent hydrodynamics; (c) generated-photon radiation and transport in the vapor cloud and nearby regions; and (d) characteristics of plasma/solid/melt-layer interactions.

The comprehensive computer simulation package high energy interaction with general heterogeneous target systems (HEIGHTS) has been developed to study in detail the various effects of sudden high-energy deposition of different sources on target materials [3]. The developed package consists of several integrated models that follow the beginning of a plasma disruption at the SOL to the transport of the eroded debris and splashed target materials as a result of the deposited energy. One model in the package, the SOLAS code, explains the plasma behavior in the SOL during a disruption and predicts the plasma parameters and conditions at the divertor plate [4]. To evaluate the magnitude of various damage mechanisms to plasma-facing and nearby components caused by plasma instabilities, we have developed full 2-D comprehensive radiation magnetohydrodynamic (MHD) models using advanced numerical techniques, such as particle-in-cell (PIC) and ray tracing methods [3]. These models with such advanced numerical methods are needed for a realistic analysis of disruption conditions and overall resulting consequences. Detailed physical models of plasma/solid–liquid/vapor interaction in a strong oblique magnetic field have also been developed, in a fully self-consistent 2-D model that is coupled with radiation MHD models. Factors that influence the lifetime of plasma-facing components, such as loss of vapor-cloud confinement and vapor removal due to MHD instabilities,

damage to nearby components from intense vapor radiation, melt splashing and brittle destruction/explosive erosion of target materials can also be modeled and studied. Fig. 2 is a schematic illustration of the various interaction zones and physics currently included in the HEIGHTS simulation package during plasma instability events.

Factors that influence the lifetime of target materials and nearby components, such as loss of vapor-cloud confinement and vapor removal due to MHD effects, damage to nearby surfaces due to intense vapor radiation, melt splashing and brittle destruction of target materials can be studied with the HEIGHTS package. Our present work focuses mainly on modeling the behavior and erosion of a metallic surface with a liquid layer subject to various internal and external forces during the energy deposition phase, as well as on the explosive erosion and on the characteristics of brittle-destruction erosion of carbon-based materials (CBMs). Lifetime predictions due to disruption erosion in a tokamak device are also presented.

It is well known that during the early stage of an intense energy deposition, a vapor cloud from the target debris will form above the bombarded surface. This shielding vapor layer, if well confined, will significantly reduce the net energy flux to the originally exposed target surface to only a few percent of its initial incident value, therefore substantially reducing the vaporization rate [1,5]. Depending on the type of application, this shielding layer can be either beneficial (i.e. the protection is desirable) or non-beneficial such as in laser or electron beam welding, cutting of materials, or protection of the earth's atmosphere and surface from colliding asteroids and comets.

The shielding efficiency of this vapor-plasma cloud will, however, depend on several factors. The net power flux reaching the target surface determines the net erosion and thus, the lifetime of plasma-facing components. Net erosion damage to PFCs due to plasma instabilities should include surface vaporization loss, erosion damage to nearby components from intense vapor radiation and macroscopic erosion from liquid–metal splashing and brittle destruction of CBMs.

2. Surface damage mechanisms

During the thermal quench phase of a tokamak plasma disruption, part of the core plasma energy ($>50\%$ of total thermal energy) is delivered from the tokamak core to the SOL and then carried to the divertor plate by energetic plasma ion and electron fluxes. Therefore, the power load to the surface is very high, reaching hundreds of GW/m^2 and is capable of causing significant damage [6]. However, because of the developed vapor cloud of surface material in the early stages of a disruption above the divertor plate, this cloud layer will shield the original surface from the incoming energy flux and significantly reduce the heat load onto the divertor plate surface. In examining the dynamics of this shielding layer, we see that after the initial phase of direct heating of divertor plate surface, a vapor cloud of the divertor surface material forms in front of the disrupting plasma and completely absorbs the incoming particle flux. As a result, the vapor cloud is heated to temperatures of up to several tens of eV [5]. At such temperatures, the vapor plasma radiation W_{rad} becomes comparable with incoming power W_{d}. Because of the absorption by a colder, denser and correspondingly more optically thick vapor plasma nearby the divertor plate surface, radiation power to the divertor plate surface is significantly decreased. Calculations with HEIGHTS predict that radiation power W_{s} onto the divertor plate surface is $<10\%$ of the original incident power because of the shielding effect [1]. The main feature of this vapor shielding layer is that W_{s} is defined by the 'temperature of ionization' T_{ion}, below which the vapor media become optically thin. Because T_{ion} depends mainly on material charge Z, the radiation power to surface W_{s} varies from 10 MW/m^2 for heavy elements, such as tungsten, to ≈ 50 MW/m^2 for light element, such as beryllium and carbon-based composites.

Models for surface vaporization, material cracking and spallation and liquid–metal ejection of melt layers have been developed for various erosion-causing mechanisms and implemented in the comprehensive HEIGHTS computer package [2–5]. Below are brief descriptions of some of the models and mechanisms used to study surface erosion and predict component lifetimes.

2.1. Erosion from surface vaporization

To evaluate the initial response of PFCs to plasma instabilities, the detailed physics of various interaction stages of plasma particles with target materials must be correctly modeled in detail. Initially, the incident plasma particles of the disrupting plasma will deposit their energy at the surface of the target material. Models for particle energy deposition and material thermal evolution were developed for multilayer structures and include phase-change and surface-vaporization models, moving boundaries, temperature-dependent thermophysical properties, etc. Deposition at higher power causes sudden and early surface vaporization of PFCs. As a result, a vapor cloud of the surface material quickly forms above the bombarded surface and in front of the incoming plasma particles. Depending on many parameters, such as incident plasma power, magnetic field structure, geometrical considerations, vapor diffusion and motion etc., the developed vapor cloud can significantly shield the original exposed areas from the incoming plasma particles and therefore, further reduce surface damage.

To calculate the efficiency of vapor-cloud shielding in protecting PFMs, detailed physics of plasma/vapor interactions have been modeled. The models include plasma particle slowdown and energy deposition in the expanding vapor, vapor heating, excitation and ionization, and vapor-generated photon radiation. The detailed vapor motion above the exposed surface is calculated by solving the vapor MHD equations for conservation of mass, momentum and energy under the influence of a strong magnetic field [7]. A significant part of the incident plasma kinetic energy is quickly transformed into vapor-generated photon radiation.

Finally, multidimensional models for photon transport throughout the expanding vapor cloud have been developed to calculate the net heat flux that reaches the original disruption surface of PFCs, as well as the radiation heat load reaching various nearby components [3]. It is the net heat flux reaching the surface that will further determine most of the response and the net erosion from surface vaporization, as well as from liquid splashing and brittle destruction of PFCs during these instabilities. The photon transport models take into account conditions for non-local thermodynamic equilibrium (non-LTE) of the vapor-cloud-generated plasma and multigroup analysis of the produced continuum and line photon spectra. Self-consistent kinetic models are also developed to calculate atoms/ions level populations and for continuum and line photon radiation transport by using advanced numerical techniques for accurate calculation of radiation propagation in the vapor cloud and in the condensed target material.

Fig. 3 shows a typical response and vapor-temperature evolution of a low-atomic number (low-Z) surface material such as lithium to a disrupting plasma incident on an inclined divertor plate. The results are presented for typical reactor disruption parameters with toroidal inclination of magnetic field lines of angle $\alpha = 10°$ and different poloidal angles, magnitude of vacuum magnetic field $B_o =$ 5 T, length of divertor plate $L \approx 20$ cm, total power of incoming plasma flux of $\approx 50–100$ GW/m^2, and particle flux of both deuterium and tritium ions, as well as electrons with similar kinetic energy of 10 keV. The spatial distribution of the incident power flux is taken as a Gaussian profile. The vapor plasma has a wide distribution of temperature: it is very hot near the front where the incident plasma particles deposit their energy and very cold near the divertor surface. The shape and the magnitude of the temperature distribution is determined by several factors: the shape of the incident disrupting plasma ions and electrons (Gaussian in this case), incident plasma power, type of vapor plasma and radiation power emitted from the vapor plasma. Higher radiation power at the front-center of the more-dense vapor plasma will tend to cool the vapor and lower its temperature in the center relative to that at the edges. For higher incident plasma power, the temperature distribution of the lithium vapor has only one peak at the center. For flat-shaped disrupting plasma, the vapor temperature is slightly peaked at the center.

Calculation of photon radiation transport in this non-LTE vapor plasma is complex, tedious and requires much computer time for reasonable

accuracy. This is quite important because the results of this calculation will determine the net radiation power flux reaching the divertor surface and other nearby components. This net power flux will eventually determine PFC erosion lifetime. Fig. 4 shows the spatial distribution of this net radiation power along the divertor plate for the initial plasma power of 100 MW/cm in the toroidal direction (i.e. 5 MW/cm^2 over 20-cm width). Radiation power W_{in} to the plate surface is given for two different divertor geometries, i.e. normal and inclined divertor plates with poloidal angles $\varphi = 0°$ and 30°, respectively. The 'wings' structure of W_s occurs only in the case of small $\varphi \approx 0°$ because of geometrical effects of radiation propagation as related to the density profile near the target surface. This results in a more homogeneous distribution of W_{in}; but for large φ, W_{in} has a maximum that is shifted to the left, i.e. to the lower edge of the divertor plate. Initially, part of the incident electron flux with high energy and large range penetrates deeply into the vapor cloud and directly reaches the edge of the divertor plate surface, where the density of the vapor cloud is lower. Therefore, total flux to the divertor plate surface, $W_{total} = W_{in} + W_{ebeam}$, is more homogeneous. Later on during the disruption, no W_{ebeam} will reach the plate surface because the vapor cloud becomes massive. It follows from the calculations that the radiation power reaching the plate surface, W_{in}, is $\approx 10\%$ of the incident total plasma power. For beryllium and carbon materials, this fraction is slightly lower and the radiation power is peaked at the center for a normal plate; because the vapor plasma is more optically thick, more radiation power is absorbed by the vapor. Thus, there is a tendency for increasing radiation power at the plate surface with decreasing atomic number for lighter elements. Because the vapor cloud is more transparent in such cases, vapor shielding is less effective and therefore, more radiation power reaches the target surface, causing

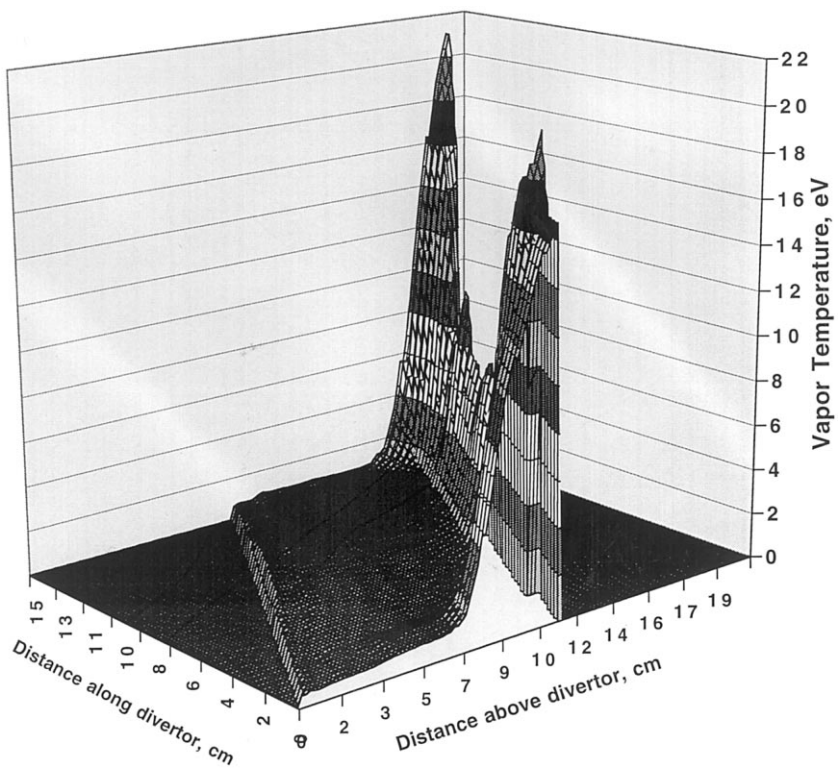

Fig. 3. Spatial evolution of vapor-cloud temperature above divertor plate during plasma instabilities.

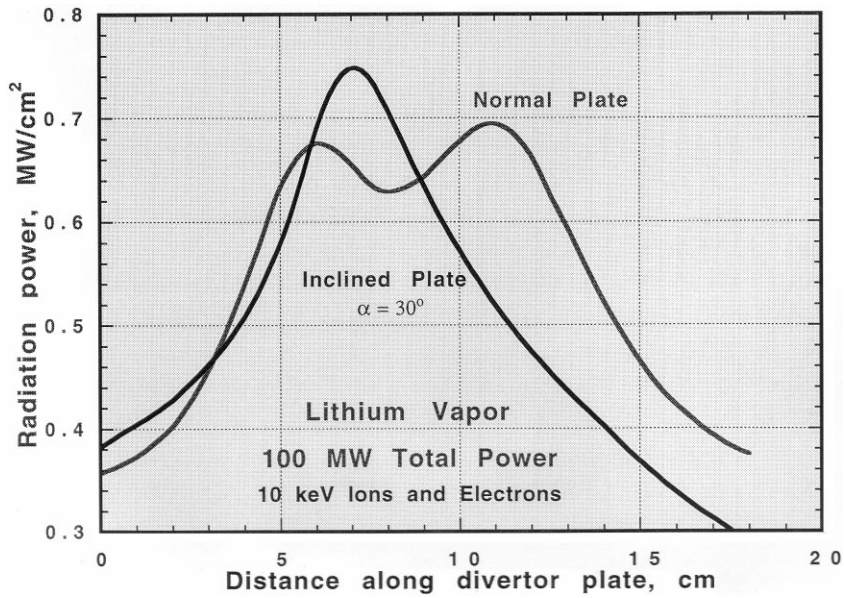

Fig. 4. Spatial distribution of net radiation power to divertor plate surface during plasma instabilities.

more splashing. The shape of the radiation power to the surface will also determine the spatial distribution of the damage profile.

2.2. Erosion mechanisms of melt layer

Radiation power reaching the target surface will result in surface vaporization and ablation, i.e. mass loss in the form of macroscopic particles. Modeling predictions have shown that surface vaporization losses of metallic materials are small (only a few tens of micrometers deep) over a wide range of plasma conditions during shorter plasma instabilities. This is due to the self-shielding mechanism discussed above in which the material's own vapor stops and absorbs most of the incoming plasma power. However, for liquid metals, surface ablation was predicted theoretically to be in the form of macroscopic metal droplets due to splashing of the molten layer [5]. Recent simulation experiments to predict erosion of candidate plasma-facing components during the thermal quench phase of a tokamak plasma disruption have also shown that erosion of metallic materials (such as W, Be, Al and Cu) can be much higher than mass losses due only to surface vaporization. These mass losses strongly depend on experimental conditions such as level of incoming power, existence of a strong magnetic field, target inclination etc. [8–11]. The mass losses are also found to be in the form of liquid metal droplets, with sizes ranging from 100 Å to tens of micrometers, leaving the target surface with velocities $V \approx 10$ m/s. Such ablation occurs as a result of splashing of the liquid layer due to several mechanisms [12]. Splashing erosion can occur due to boiling and explosion of gas bubbles in the liquid, absorption of plasma momentum, hydrodynamic instabilities developed in the liquid layer from various forces, runoff of melt layers over the structure and mechanical vibration of the machine during the disruption. One main mechanism of splashing results from the hydrodynamic instabilities developed in the liquid surface (such as Kelvin–Helmholtz and Rayleigh–Taylor instabilities). It was shown that Kelvin–Helmholtz instability can occur if the vapor plasma is not well confined by the magnetic field and vapor flow occur along the target surface [13]. Another splashing mechanism that was predicted theoretically [5] and proved experimentally [14] is from volume bubble boiling. This usually occurs from overheating of the liquid metal above

the vaporization temperature T_v, i.e. the temperature at which saturation pressure is equal to the outer pressure of the vapor plasma above the divertor plate surface. Therefore, the erosion energy is roughly equal to the sum of the thermal energy (required to heat the liquid above a certain temperature, i.e. melting temperature for hydrodynamic instabilities and vaporization temperature for bubble boiling), melting energy (i.e. heat of fusion), and kinetic energy of the droplets. The kinetic energy of the splashed droplets is determined from the surface tension of the liquid metal.

To correctly predict melt-layer erosion, a four-moving-boundaries problem is solved in the HEIGHTS package. The front of the vapor cloud, generated from the initial plasma power deposition, is one moving boundary determined by solving vapor hydrodynamic equations. The second moving boundary due to surface vaporization of the target is calculated from target thermodynamics. Immediately following the surface vaporization front is a third moving boundary due to the melt-splashing front. Finally, the fourth moving boundary is at the liquid/solid interface, which further determines the new thickness of the melt layer. These moving boundaries are interdependent, and a self-consistent solution must link them dynamically and simultaneously. It is the third moving boundary (the liquid splashing front), however, that determines the extent of metallic PFC erosion and lifetime due to plasma instabilities. The SPLASH code, part of the HEIGHTS package, calculates mass losses by using a splashing-wave concept as a result of each erosion-causing mechanism [15]. Thus, total erosion can be calculated from the sum of all possible erosion mechanisms.

2.3. Erosion mechanisms of carbon-based-materials

Non-melting materials, such as graphite and CBMs, have also shown large erosion losses significantly exceeding that from surface vaporization. This phenomenon has been observed in different disruption simulation facilities such as electron beams [16], laser [17], plasma guns and other devices [18]. Models were developed to evaluate erosion behavior and lifetime of CBMs of plasma facing and nearby components due to brittle destruction during plasma instabilities [3].

The macroscopic erosion of CBMs depends on three main parameters: net power flux to the surface, exposure time and threshold energy required for brittle destruction. The required energy for brittle destruction is critical in determining the net erosion rate of CBMs and is currently estimated from disruption-simulation experiments. From these experiments, the energy for brittle destruction of graphite similar to the MPG-9 graphite is estimated to be ≈ 10 kJ/g, or 20 kJ/cm^3 [18]. Therefore, for a net power flux to the material surface during the disruption of ≈ 300 kW/cm^2, the deposited energy for a time of 1 ms is ≈ 0.3 kJ/cm^2, which results in net erosion of ≈ 150 μm per disruption. This value is much higher than that predicted from pure surface vaporization of ≈ 10 μm per disruption for CBMs [10]. A sacrificial coating/tile thickness ≈ 1 cm thick would last < 70 disruptions. Again, this is far less than the current expectation of several hundred disruptions during the reactor lifetime. Longer disruption times can also significantly reduce disruption lifetime. Therefore, more relevant experimental data and additional detailed modeling are needed to evaluate the erosion of CBMs, which strongly depends on the type of carbon material.

3. Droplets shielding concept

Complete and accurate calculation of mass losses during plasma instabilities requires a full MHD description of the vapor media near the target surface that consists of a mixture of vapor and droplets moving away from surface. Photon radiation power from the upper vapor regions will then be absorbed by both the target surface and the droplet cloud. This will result in the surface vaporization of both target and droplet surfaces. Therefore, in such a mixture of erosion products, further screening of the original target surface takes place due to the splashed droplets or macroscopic debris of CBMs. This has the effect of

reducing photon radiation power to target surface. Such screening can be called 'droplet shielding' in an analogy to the vapor shielding effect. Fig. 5 is a schematic illustration of the droplet and macroscopic shielding concept during plasma/material interaction following a plasma instability. Features of this droplet shielding and its influence on total mass loss are given below for the cases of volume bubble boiling with homogeneous velocities of droplets in momentum space and Rayleigh–Taylor instability with droplets that move normal to the surface preferentially.

The emitted macroscopic particles usually have a distribution that depends on their size and velocity. We will initially consider particles with an average radius R_d and an average velocity V in the normal direction. Heat conduction from the vapor to macroscopic particles will be neglected; therefore, these particles are heated only by radiation. Due to absorption of radiation by the particles, the radiation flux W_s that reaches the divertor plate surface will be lower than the total radiation flux W_{in} that is arriving from longer distances near the hotter vapor, where the radiation that can reach the target surface originates, i.e. $W_s < W_{in}$. Part of the radiation flux reaching the surface is spent for vaporization and liquid ablation, i.e. macroscopic-particle formation. Because the vaporization energy per gram is much higher than the required energy for ablation, mass losses due to splashing/brittle destruction are much larger than mass loss from surface vaporization. Most radiation power reaching the target surface is then spent in splashing and macroscopic particle formation.

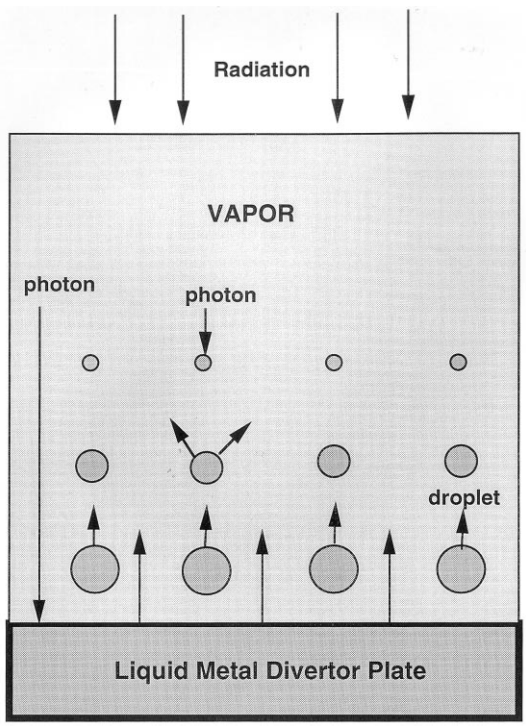

Fig. 5. Schematic illustration of droplet and macroscopic shielding concept during plasma/material interaction following plasma instabilities.

HEIGHTS package calculations showed that radiation power to the surface decreased about five times due to droplet shielding in the case of lithium as the PFM. It is also concluded that W_s does not depend on initial parameters of macroscopic particles, such as initial radius R_{d0} and velocity U, which are not well defined. This means that the droplet shielding effect does not depend on size and velocity distributions of the droplets but only on energies of ablation destruction and vaporization. Therefore, this consideration is valid for any arbitrary distribution of droplet velocities in momentum space for the studied conditions.

To summarize the simulation results, due to overheating of the divertor plate surface, macroscopic particles and droplets are ejected/splashed upstream and away from the surface. These particles then absorb some part of the incoming vapor radiation. The net fraction of radiation power reaching the divertor plate surface is determined only by the ratio of vaporization to splashing or brittle destruction energies. The distance at which macroscopic particles are completely vaporized is calculated to be ≈ 100 times the initial radius of droplets. Because the initial droplet radius is small (≤ 10 μm), the droplets completely vanish at distance $L \leq 1$ cm. Therefore, the mixture of vapor and macroscopic particles exists only very near the divertor plate surface. Most incoming radiation power from the upper vapor cloud regions is spent in heating and vaporization of the macroscopic particles. Therefore, in spite of initial large

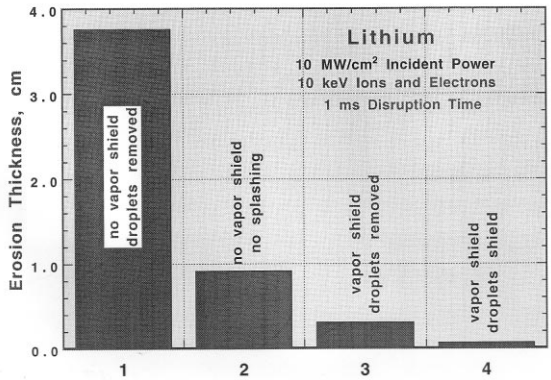

Fig. 6. Effect of vapor-cloud stability and macroscopic particle/droplet shielding on total mass loss during a disruption.

splashing erosion, total erosion of the divertor plate is defined only by vaporization losses including both divertor plate vaporization and macroscopic-particle vaporization. Again, this is true only if both the vapor cloud and the splashed droplets and macroscopic particles are well confined in front of the disrupting plasma.

Nonhomogenous velocity distribution of droplets in momentum space can exist during Kelvin–Helmholtz hydrodynamic instabilities that arise when the vapor-plasma wind along the divertor surface exist as a result of MHD turbulence in the distorted oblique magnetic field lines. For this case, a corresponding model has been developed to account for macroscopic particle lifetime in the vapor cloud. This is now implemented in the SPLASH code, where the dynamics of such mixture is treated simultaneously in detail.

4. Total mass loss of target plate

It follows from the above discussions that vapor shielding results in a strong decrease of power that reach the surface from incoming plasma power of $W_d = 50–100$ GW/m^2 to $W_s < 10$ GW/m^2. The droplet-shielding effect further reduces the net incoming power to divertor surface through droplets and macroscopic particle vaporization. This will have the overall effect of significantly reducing mass losses in a disruption event. Such reduced value of mass losses does not appear to be excessive because the depth of liquid flow defined by heat removal requires a thickness greater than ≈ 1 cm. It is interesting to compare this mass loss with the mass losses with and without both vapor shielding and droplet shielding, as shown in Fig. 6. In case 1, i.e. in the absence of both shielding mechanisms (no vapor shielding, i.e. vapor is not well confined and no droplets shielding, so that droplets are splashed away from the incoming plasma), all incoming power will be spent in splashing erosion of the liquid surface. Erosion loss is very high and this case may represent a disruption simulation device in which the incident plasma has a very high dynamic pressure that is capable of blowing off the initial vapor cloud and liquid layers. In case 2 without the vapor shielding and splashing (or brittle destruction), all incoming power will be spent in vaporizing the target surface. This may occur if the vapor cloud is removed for any reason and the target material does not melt or splash/destruct. In case 3 with vapor shielding but without droplet shielding (droplets are removed away from incoming power), the net incoming radiation power to target surface is spent in splashing. This situation can occur on nearby components during a disruption on the divertor plate, in which the intense photon radiation from the hot vapor cloud deposits its power at the locations having different orientations to the magnetic field lines, as a result, the vapor cloud is not well confined. This may also be true in many of the disruption simulation devices such as plasma guns and electron beams, in which the sample size is small and the droplets or macroscopic particles do not have enough time to absorb the incoming radiation power and shield the target surface. Therefore, a well-confined vapor and droplet cloud can reduce erosion losses by up to two orders of magnitude. However, droplets and macroscopic particles that are ejected near target edges and/or having larger sizes or moving with higher velocities will not have sufficient time to completely vaporize and shield the target surface; therefore resulting in lower erosion lifetime.

In summary, erosion of the divertor plate associated with shielding by both vapor and droplets

clouds may not seem to be very high and therefore, divertor erosion due the thermal quench phase of a tokamak plasma disruption may not be the main life-limiting issue for the divertor system. Of course, this conclusion is valid only when the vapor plasma is well confined by the oblique magnetic field. However, loss of vapor confinement can occur if the balloon mode of the MHD flute instability arises due to distortion of the oblique magnetic field lines by the expanding vapor plasma [19]. In this case, arising turbulence results in vapor flow along the divertor plate surface. Due to this flow, first, the Kelvin–Helmholtz instability of unstable surface waves arises that results in splashing. Second, this vapor flow blows away both vapor and droplets along the target surface. This second phenomenon reduces vapor-shielding efficiency because of vapor cloud removal; in addition, efficiency of droplet shielding is reduced due to decreased droplet exposure time in the depleted vapor.

Fig. 7 shows the predicted maximum tolerated number of disruptions for a beryllium PFM as a function of disruption time in reactor conditions for the case of full vapor shielding but with and without the droplet shielding effect, and an incident plasma power of 10 MW/cm^2. The initial thickness of beryllium-facing material is assumed to be 5 mm, of which 50% is to be sacrificed to disruption erosion. The tolerated number of disruptions becomes unacceptable at longer disruption times and if no macroscopic particle/droplets shielding occurs. No droplet shielding can be expected if the vapor cloud is not well confined or during erosion of nearby components from the intense photon radiation on the vapor cloud in a closed divertor configuration. Greater initial thickness of PFMs will increase erosion lifetimes. The maximum initial thickness is limited, however, by the maximum allowable surface temperature that depends on normal operating conditions and on material constraints.

The existence of vapor shielding that protects the divertor plates from high heat loads means that $>90\%$ of incoming power is radiated to nearby locations. Therefore, the problem of erosion of other parts in a closed divertor system becomes more serious. It was shown both theoretically [20] and experimentally [21] that interaction of this 'secondary' radiation with other components results in the same consequences as the primary interaction of the SOL plasma, i.e. vapor cloud formation, splashing, etc. Moreover, it may be very difficult for such vapor clouds to be well confined especially if the magnetic field angle of inclination with different oriented surfaces is very small. Erosion of such nearby components can be estimated as in case 1, shown in Figs. 6 and 7, because of the absence of both shielding effects.

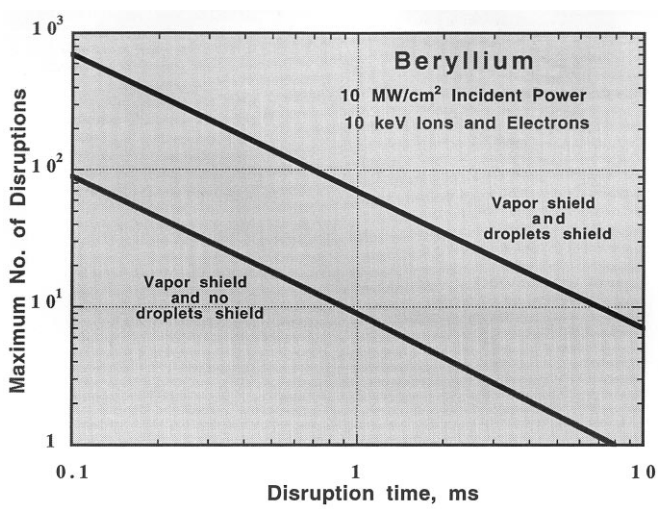

Fig. 7. Maximum tolerated number of disruptions depending on stability of vapor cloud and droplet shielding and confinement.

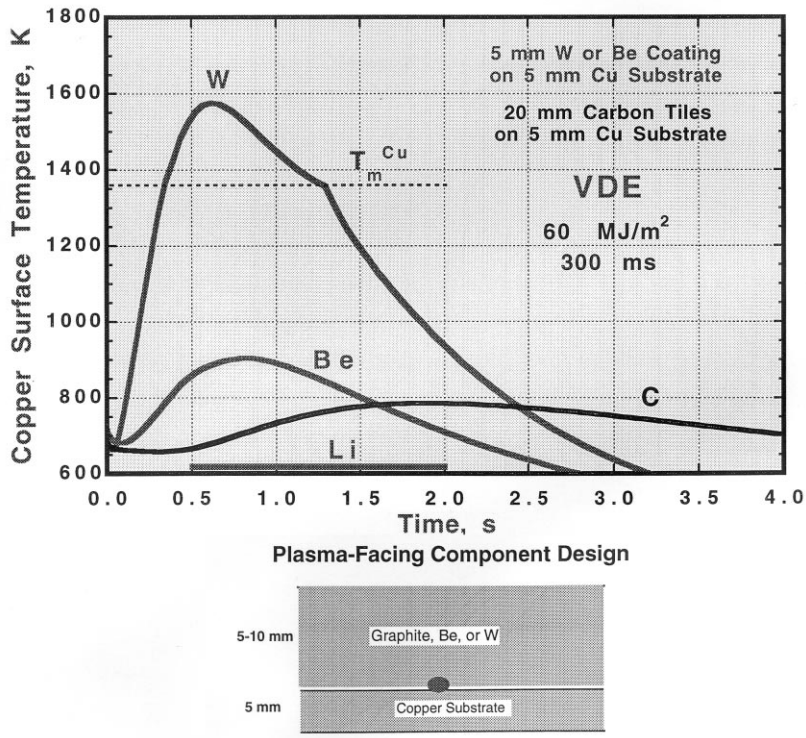

Fig. 8. Rise in copper surface temperature of carbon-, beryllium-, tungsten- and lithium-coated copper substrates during a VDE.

During the thermal phase of a tokamak plasma disruption, redeposition of the eroded liquid surfaces due to vaporization and splashing or macroscopic particles will occur. As a result, all inner surfaces of the divertor system can be covered by a layer of the liquid metal surface that is condensed from vapor atoms and resolidified liquid droplets or macroscopic particles. A procedure to clean up the dust and redeposited debris of the eroded materials is just as important as the procedure to repair the incurred damage on PFCs. Therefore, it is a good idea to fabricate or cover all vapor-facing materials with the same liquid metal that is used initially.

5. Bulk damage effects

Although thermal-quench disruptions have no significant thermal effect on structural materials and coolant channels, VDEs, in addition to causing severe surface melting and erosion, can result in substantial damage to these components [1]. Because of the longer deposition time of VDEs (100–300 ms), much of the plasma incident energy will be conducted through the surface coating material onto the copper structural material and finally, to the coolant channels. One concern is the higher temperature observed in the structural material, particularly at the interface with the coating materials. Higher temperatures cause high thermal stresses in the structure and seriously degrade the integrity of the interface bonding because of thermal diffusion and formation of intermetallic compounds, which may lead to detachment of the coating from the structural material. Fig. 8 shows temperatures, during a typical VDE, of a copper surface at its interface with tungsten or beryllium coatings of 5 mm thickness and with 20-mm-thick carbon tiles over a 5 mm copper substrate. Surface coating and tile thickness is determined by the surface temperature

limitations during normal operation. For reactor Demo-like conditions, the thickness of a beryllium or tungsten divertor target is usually < 10 mm. Thinner coatings are also desirable because of cost, safety and concern about plasma contamination. Tungsten and carbon coatings of similar thicknesses usually result in similar and higher copper surface temperatures than that of a beryllium coating because most of the incident plasma energy is removed by the beryllium's higher surface vaporization rate, leaving little energy to be conducted through the structural material [1]. In the case of a 5-mm-thick tungsten coating, the copper surface interface actually melts. Only beryllium coatings of reasonable thickness (< 5–10 mm) or very thick carbon tiles (> 20 mm) can withstand the acceptable temperature rise in the copper structure for the conditions shown. However, beryllium and carbon coating materials will suffer significant surface erosion in order to protect the structural copper substrate. A thin free-surface layer of a liquid metal, such as lithium of ≈ 1 cm thick, will be an ideal solution to completely protect the structure and to offer unlimited PFC erosion lifetime. The copper structure during the VDE will have no temperature rise (as shown in Fig. 8) because the lithium will remove the heat either by convection (moving film) or by vaporization (stationary film). However, issues related to plasma/free-surface liquid–metal interactions during normal operations must be carefully examined.

6. Conclusions

Various effects of plasma/material interactions during plasma instabilities, such as disruptions and vertical displacement events, have been studied with a comprehensive HEIGHTS dynamic model package that integrates in fine detail the structure's thermal evolution, physics of plasma/vapor interactions, magnetohydrodynamics and photon radiation transport of multilayer structures. Various plasma instabilities result in different damage to plasma-facing and structural materials. Models and theories are developed for material erosion during intense deposition of energy on target surfaces. Vapor and droplet shielding effects are both very important in reducing disruption erosion effects. Theoretical predictions of HEIGHTS package are generally in good agreement with current simulation experiments. The use of a renewable material, such as free-surface liquid lithium, may significantly extend the lifetime of PFMs and substantially enhance the tokamak concept for power production reactors. More-detailed modeling and more reactor-relevant simulation experiments are required before a final recommendation is made for the selection of PFMs. In general, plasma instabilities must be avoided or sharply minimized. Moreover, the effects of redeposited debris from the eroded materials on plasma contamination and on subsequent reactor operations must be further studied.

Acknowledgements

This work is supported by the US Department of Energy, Office of Fusion Energy Sciences, under Contract W-31-109-Eng-38.

References

[1] A. Hassanein, Fusion Technol. 30 (1996) 713.
[2] A. Hassanein, G. Federici, I. Konkashbaev, et al., Fusion Eng. Des. 39–40 (1998) 201.
[3] A. Hassanein, I. Konkashbaev, J. Nucl. Mater. 273 (1999) 326.
[4] A. Hassanein, I. Konkashbaev, Physics of Collisionless Scrape-Off-Layer Plasma During Normal and Off-Normal Tokamak Operating Conditions, Argonne National Laboratory Report ANL/FPP/TM-296, March, 1999.
[5] A. Hassanein, I. Konkashbaev, Suppl. J. Nucl. Fusion 5 (1994) 193.
[6] A. Hassanein, Response of Materials to High Heat Fluxes During Operation in Fusion Reactors, ASME, 88-WA/NE-2, 1988.
[7] A. Hassanein, I. Konkashbaev, Fusion Eng. Des. 28 (1995) 27.
[8] V. Belan, V. Levashov, V. Maynashev, et al., J. Nucl. Mater. 233–237 (1996) 763.
[9] V. Litunovsky, V. Bakhtin, S. Kurkin, et al., in: B. Beaumont, P. Libeyre, B. de Gentile, G. Tonon (Eds.), Fusion Technology, 1998, p. 59.
[10] A. Hassanein, I. Konkashbaev, J. Nucl. Mater. 233–237 (1996) 713.

[11] N.I. Arkhipov, V. Bakhtin, S. Kurkin, et al., J. Nucl. Mater. 233–237 (1996) 767.
[12] A. Hassanein, Fusion Technol. 15 (1989) 513.
[13] V. Litunovsky, I. Ovchinnikov, A. Drozdov, et al., Proceedings of the Sixteenth IEEE/NPSS Symposium on Fusion Engineering, September 30 to October 5, 1995, p. 435.
[14] T. Burtseva, et al., Plasma Dev. Operat. 4 (1995) 31.
[15] A. Hassanein, A. Konkashbaev, I. Konkashbaev, in: K. Herschbach, W. Maurer, J.E. Vetter (Eds.), Fusion Technology, 1994, p. 223.
[16] J. Linke, et al., in: B. Keen, M. Huguet, R. Hemsworth (Eds.), Fusion Technology, 1991, p. 428.
[17] J. Van der laan, J. Nucl. Mater. 162–164 (1989) 964.
[18] A.V. Burdakov, M. Chagin, V. Filippov, et al., J. Nucl. Mater. 233–237 (1996) 697.
[19] A. Hassanein, I. Konkashbaev, Plasma Dev. Operat. 5 (1998) 297.
[20] A. Hassanein, I. Konkashbaev, in: C. Varandas, F. Serra (Eds.), Fusion Technology, 1996, p. 379.
[21] V. Safronov, N. Arkhipov, V. Bakhtin, et al., in: B. Beaumont, P. Libeyre, B. de Gentile, G. Tonon (Eds.), Fusion Technology, 1998, p. 105.